LETTER

doi:10.1038/nature13892

Asymmetric photoredox transition-metal catalysis activated by visible light

Haohua Huo[1], Xiaodong Shen[1], Chuanyong Wang[1], Lilu Zhang[1], Philipp Röse[1], Liang-An Chen[2], Klaus Harms[1], Michael Marsch[1], Gerhard Hilt[1] & Eric Meggers[1,2]

Asymmetric catalysis is seen as one of the most economical strategies to satisfy the growing demand for enantiomerically pure small molecules in the fine chemical and pharmaceutical industries[1]. And visible light has been recognized as an environmentally friendly and sustainable form of energy for triggering chemical transformations and catalytic chemical processes[2–5]. For these reasons, visible-light-driven catalytic asymmetric chemistry is a subject of enormous current interest[2–5]. Photoredox catalysis provides the opportunity to generate highly reactive radical ion intermediates with often unusual or unconventional reactivities under surprisingly mild reaction conditions[6]. In such systems, photoactivated sensitizers initiate a single electron transfer from (or to) a closed-shell organic molecule to produce radical cations or radical anions whose reactivities are then exploited for interesting or unusual chemical transformations. However, the high reactivity of photoexcited substrates, intermediate radical ions or radicals, and the low activation barriers for follow-up reactions provide significant hurdles for the development of efficient catalytic photochemical processes that work under stereochemical control and provide chiral molecules in an asymmetric fashion[7]. Here we report a highly efficient asymmetric catalyst that uses visible light for the necessary molecular activation, thereby combining asymmetric catalysis and photocatalysis. We show that a chiral iridium complex can serve as a sensitizer for photoredox catalysis and at the same time provide very effective asymmetric induction for the enantioselective alkylation of 2-acyl imidazoles. This new asymmetric photoredox catalyst, in which the metal centre simultaneously serves as the exclusive source of chirality, the catalytically active Lewis acid centre, and the photoredox centre, offers new opportunities for the 'green' synthesis of non-racemic chiral molecules.

Recently, strategies have been developed in which efficient catalytic photochemical processes that work under stereochemical control and provide chiral molecules in an asymmetric fashion can be carried out by two catalysts that work in tandem for a single chemical transformation[8]. In such dual-catalyst reactions, visible-light redox sensitizers are combined with asymmetric co-catalysts, such as chiral secondary amines[9–13], chiral *N*-heterocyclic carbenes[14], chiral Brønsted acids[15], chiral Lewis acids[16], or chiral thiourea[17]. With respect to single catalysts, ultraviolet light in combination with hydrogen bonding or Lewis acid interaction has been used previously in pioneering work to trigger enantioselective catalysis[18–20], and an enantioselective cycloaddition induced by visible light—although not including photoinduced electron transfer—has been reported[21]; also, an interesting but special case of photoactivated enamine catalysis was disclosed recently in which a transient electron donor–acceptor complex is capable of absorbing visible light and triggering a charge transfer[22]. General solutions for interfacing visible-light-induced photoredox chemistry and asymmetric catalysis with single catalysts are highly desirable, and will potentially provide new opportunities for reaction design by having a closer control over the entire reaction path, including the crucial stereodiscrimination step.

Taking into account that currently used visible-light photosensitizers are typically based on transition-metal complexes[2–5], and that chiral transition-metal complexes constitute an established class of catalysts for asymmetric transformations[1], we envisioned the combination of these two features into a single transition-metal-based asymmetric photoredox catalyst. We conducted our study with the recently developed chiral-at-metal iridium(III) complex Λ-**Ir1**[23] and the derivative Λ-**Ir2** (Fig. 1). In both complexes, the octahedral iridium centre is coordinated by two achiral bidentate ligands in a left (Λ)- or right (Δ)-handed propeller-type fashion, thereby establishing metal-centred chirality[24,25], and coordinated by two additional labile acetonitriles which give access to a Lewis acid metal centre upon ligand exchange (see Supplementary Fig. 1 for a crystal structure of Λ-**Ir2**). Our laboratory has previously reported the activation of α,β-unsaturated 2-acyl imidazoles by chiral-at-metal Λ- or Δ-**Ir1** as a step towards the enantioselective addition of indole nucleophiles[23], so we considered the possibility that these chiral Lewis acids might be capable of intertwining chiral enolate catalysis[26] with photoredox radical ion chemistry[2–5]: we therefore selected the model reaction of 2-acyl imidazole **1a** with the electron deficient benzyl bromide **2a** as our starting point (see Table 1). Encouragingly, in the presence of light from a 14 W energy-saving household lamp, Λ-**Ir1** at a loading of 5 mol% was able to catalyse the reaction between **1a** and **2a**, providing the α-alkylation product **3a** in good yield (85%) and with high enantioselectivity (95% enantiomeric excess, e.e.) after 20 h photolysis at room temperature (entry 1 of Table 1). Optimization of the reaction conditions—by empirically adjusting the solvent, increasing the concentration to speed up the reaction, slightly raising the temperature to promote ligand exchange at the iridium centre, and adding the weak base Na_2HPO_4 to facilitate enolate chemistry—provided the product **3a** in an excellent yield of 97% with 95% e.e. after exposure to visible light for just 3 h in the presence of a reduced catalyst loading of just 2 mol% Λ-**Ir1** (entry 2). The catalyst Λ-**Ir2** (2 mol%) even provided the α-alkylation product in quantitative yield with a superior enantioselectivity of 99% e.e. and a further reduced reaction time of 1.5 h (entry 3). We attribute the improved enantioselectivity to an increased steric hindrance in Λ-**Ir2** compared to Λ-**Ir1** created by the long C–S bonds of the benzothiazole moieties, which position the two *tert*-butyl groups somewhat closer to the exchange-labile acetonitrile ligands (see Supplementary Fig. 2). The loading of the

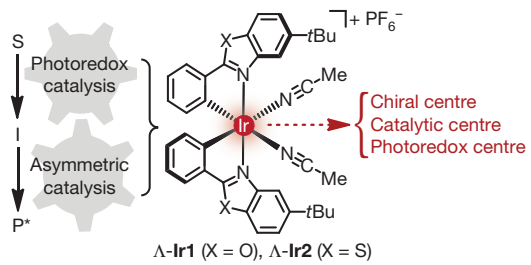

Figure 1 | Chiral iridium complexes for asymmetric photoredox catalysis. S, substrate; I, intermediate; P*, non-racemic chiral product. The Ir centre acts as a chiral centre, a catalytic centre, and a photoredox centre.

[1]Fachbereich Chemie, Philipps-Universität Marburg, Hans-Meerwein-Straße, 35043 Marburg, Germany. [2]College of Chemistry and Chemical Engineering, Xiamen University, Xiamen 361005, China.

Table 1 | Initial iridium-catalysed photoinduced enantioselective alkylation of acyl imidazole 1a with benzyl bromide 2a

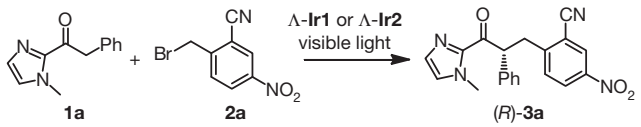

Entry	Catalyst	Illumination*	Reaction conditions†	*t* (h)	Yield‡ (%)	e.e.§ (%)
1	Λ-**Ir1** (5 mol%)	Visible light	**1a** (0.3 M, 3 equiv.), MeOH, RT	20	85	95
2	Λ-**Ir1** (2 mol%)	Visible light	Na_2HPO_4, **1a** (1.2 M, 3 equiv.), MeOH/THF (4:1), 40 °C	3	97	95
3	Λ-**Ir2** (2 mol%)	Visible light	Same as above	1.5	100	99
4	Λ-**Ir2** (0.5 mol%)	Visible light	Same as above	4.5	97	98
5	Λ-**Ir2** (2 mol%)	Dark	Same as above	1.5	<5	ND
6	None	Visible light	Same as above	16	0	NA

RT, room temperature; ND, not determined; NA, not applicable.
* Light source: 14 W white light energy-saving lamp.
† All reactions performed under the exclusion of air. See Supplementary Methods for more details.
‡ Isolated yields.
§ Enantiomeric excess determined by HPLC analysis on chiral stationary phase.

catalyst Λ-**Ir2** can be further decreased to merely 0.5 mol% without much affecting the yield (97%) or the enantioselectivity (98% e.e.) (entry 4). We note that neither the catalyst Λ-**Ir2** alone in the dark (entry 5) nor visible light in the absence of the catalyst (entry 6) trigger this reaction to a significant degree under these conditions, thus unequivocally demonstrating that it is the combination of iridium(III) complex and visible light that is necessary to efficiently catalyse the enantioselective C–C bond formation.

Examples of the photoinduced enantioselective α-alkylation of 2-acyl imidazoles with benzyl bromides catalysed by Λ-**Ir2** are summarized in Fig. 2. A variety of electron acceptor substituted benzyl bromides provide the α-alkylation products in up to quantitative yields (97–100%) and with up to almost perfect enanantioselectivities (94–99% e.e.), while requiring only short reaction times of 1.5 to 6 h (**3a**–**d**). The 2-acyl-*N*-methylimidazole substrates tolerate steric (products **3e** and **3f**), electron donating (product **3g**) and electron accepting (product **3h**) substituents in the phenyl moiety, which can be replaced by the bicyclic aromatic naphthalene (product **3i**) or the heteroaromatic thiophene (product **3j**). Furthermore, the photoredox catalysed reaction also tolerates less acidic 2-acyl-*N*-methylimidazoles devoid of any aromatic substituent at the methylene group, as demonstrated for the products **3k** and **3l**. For these substrates, the addition of a weak base is essential to achieve high conversions and excellent enantioselectivities. We also tested a different class of electrophiles, namely phenacyl bromides, and found that they readily provide the expected C–C bond formation products with very good yields of 86–91% and high enantioselectivities of 90–91% e.e. (products **3m**–**o**). In order to reach satisfactory enantioselectivities, the *N*-methyl substituent at the imidazole moiety needed to be replaced by the more bulky isopropyl group. Overall, it can be concluded that Λ-**Ir2** is a highly effective catalyst for the α-alkylation of acyl imidazoles with acceptor substituted benzyl bromides and phenacyl bromides in the presence of visible light with high to quantitative yields and impressive enantioselectivities, while only using a catalyst loading of 2 mol%.

A plausible mechanism in which photoredox catalysis intertwines with asymmetric catalysis is shown in Fig. 3. Herein, the catalysis is initiated by the coordination of 2-acyl imidazoles (**1**) to the iridium catalyst in a bidentate fashion (intermediate **I**), followed by the formation of a nucleophilic iridium(III) enolate complex (intermediate **II**) upon deprotonation. The subsequent chirality generating key step constitutes the exergonic addition of a photo-reductively generated electrophilic radical to the electron rich metal-coordinated enolate double bond, thereby affording an iridium-coordinated ketyl radical (intermediate **III**). Oxidation of this ketyl intermediate to a ketone by single electron transfer regenerates the iridium(III) photosensitizer and provides the iridium-coordinated product (complex **IV**), which is released upon exchange with unreacted starting material, followed by a new catalytic cycle. The proposed key intermediate which uniquely connects the asymmetric catalysis with the photoredox cycle is the iridium(III) enolate complex **II**, which not only provides the crucial asymmetric induction in the catalysis cycle and but at the same time serves as the *in situ* generated active chiral photosensitizer[27].

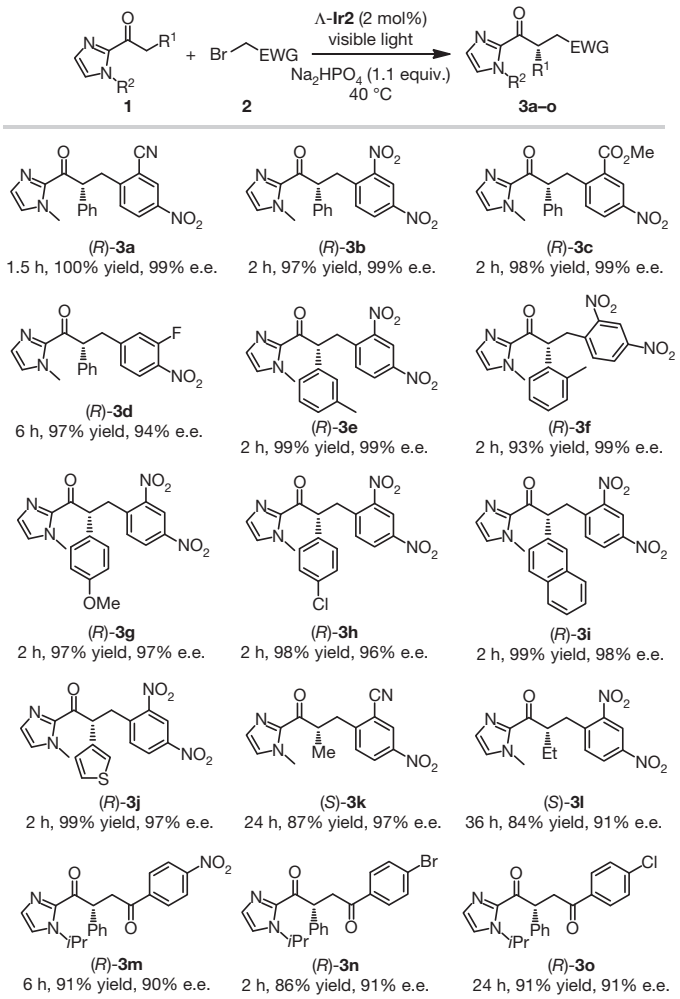

Figure 2 | Substrate scope of the photoinduced enantioselective alkylation of 2-acyl imidazoles with acceptor substituted benzyl bromides and phenacyl bromides. Top row, the studied reaction; all other rows show products, giving reaction time, isolated yields after chromatographic purification, and enantiomeric excess (e.e.), which was determined by HPLC on a chiral stationary phase. Product (*S*)-**3k**: for comparison, in the absence of base a yield of 18% with 91% e.e. was obtained after photolysis for 24 h. Product (S)-**3l**: reaction was irradiated instead with a blue LED light source (3 W) in order to improve the yield. EWG, electron withdrawing group.

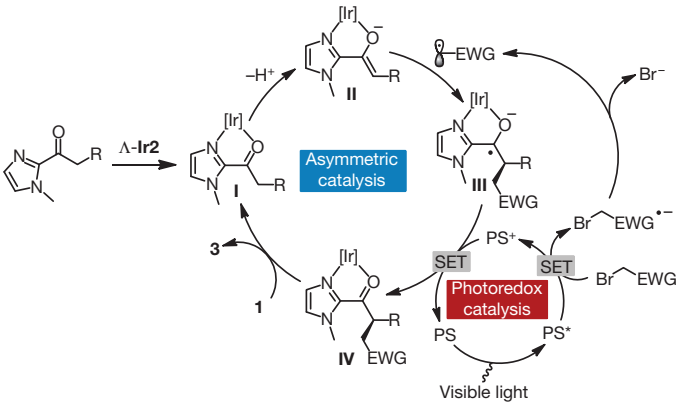

Figure 3 | Plausible mechanism for a combined photoredox and asymmetric catalysis. For variations of this mechanism, see Supplementary Fig. 7. SET, single electron transfer; EWG, electron withdrawing group; PS, photosensitizer in the form of enolate complex **II**. See main text for details.

A series of investigations support this mechanism. To start with, as confirmed by X-ray crystallography (Supplementary Fig. 3), 2-acyl-*N*-methylimidazoles efficiently coordinate to the iridium catalyst Λ-**Ir2** in a bidentate fashion upon release of the two monodentate acetonitrile ligands, thereby providing the proposed intermediate complex **I**. Subsequent deprotonation generated the intermediate iridium(III) enolate complex **II**, which was independently isolated and unambiguously characterized by X-ray crystallography, as shown in Fig. 4a. This structure also illustrates that one face of the prochiral enolate π-bond is blocked by a *tert*-butyl group, thereby rationalizing the observed high asymmetric induction in the course of the proposed diastereoselective addition of the electron-deficient radical to the electron-rich double bond[28]. The determined absolute configurations of the α-alkylation products are consistent with this mechanistic picture. This reaction step relates to recent reports of the photosensitized generation of electron-deficient radicals and their stereoselective addition to electron-rich π systems of chiral enamines[9–13]. For our system, a radical mechanism is consistent with the observation that photoreactions in the presence of air, the alkene 1,1-diphenylethylene (isolation of adduct **4**) or the radical trap 2,2,6,6-tetramethylpiperidine-1-oxyl (TEMPO) (isolation of products **5** and **6**) suppress the formation of the α-alkylation product (Fig. 4b). Furthermore, the direct correlation between photolysis and product formation is demonstrated by a light–dark interval reaction shown in Fig. 4c.

Importantly, several experimental results lead to the conclusion that the intermediate iridium(III) enolate complex **II** is not only a key nucleophilic intermediate in the asymmetric catalysis cycle, but also constitutes the active *in situ* assembled photosensitizer in the photoredox cycle. Since iridium(III) complex **II** apparently represents the only neutral iridium(III) complex within the reaction mixture, this conclusion is also consistent with observed trends regarding redox and photophysical properties of iridium(III) complexes—namely that neutral *bis*-cyclometalated iridium(III) photosensitizers are significantly stronger photoreducing agents than their cationic counterparts[4]. Accordingly, Stern–Volmer plots (Fig. 4d) illustrate that the luminescence emission of the enolate complex **II** is quenched by benzyl bromide **2a** much more efficiently compared to **Ir2**, which can be attributed to a fast electron transfer from a triplet excited state of enolate complex **II** to the electron-deficient benzyl bromide. This is furthermore supported by cyclic voltammetry (Supplementary Fig. 4), which reveals that the enolate complex **II** has a significantly decreased oxidation potential (by around 1 V) compared to the cationic complex **Ir2**, and thus comprises a much stronger reducing agent in the ground state and even more so in its photoexcited state (Fig. 4e). The estimated excited state redox potential $E_{1/2}(\mathbf{II}^+/\mathbf{II}^*)$ of −1.74 V versus Ag/AgCl for the enolate complex **II** is comparable to that of *fac*-[Ir(ppy)$_3$] (ppy = 2-phenylpyridine)[4], an iridium sensitizer that has been used previously for the reductive cleavage of electron deficient benzyl bromides[10]. Conveniently, compared to **Ir2** and established iridium(III) photosensitizers[4], the enolate complex **II** displays a bathochromically shifted long wavelength absorbance maximum with an additional shoulder at around 500 nm, thus permitting an excitation

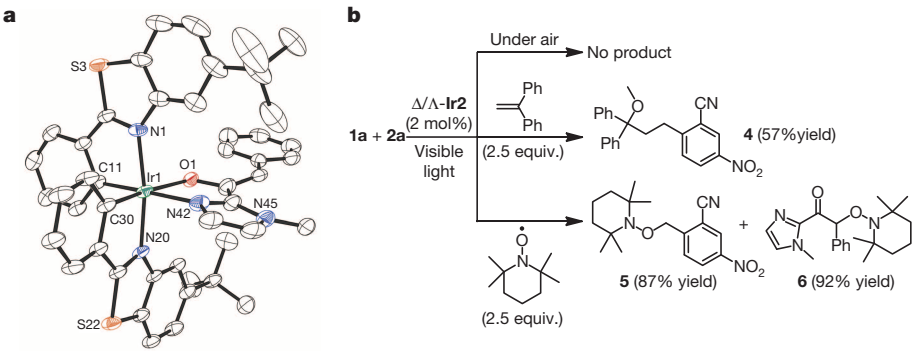

Figure 4 | Mechanistic investigations. **a**, X-ray crystal structure of the proposed Ir(III) enolate complex intermediate **II**. This compound was crystallized as a racemic mixture, and only the Λ-enantiomer is shown here, as an ORTEP drawing with 30% probability ellipsoids. **b**, Control experiments in the presence of molecules which react with radicals. See main text for details. **c**, Light–dark interval experiment for the reaction **1a** + **2a** → **3a** according to entry 3 of Table 1. **d**, Luminescence quenching experiments. I_0 and I are respectively luminescence intensities in the absence and presence of the indicated concentrations of the electron deficient benzyl bromide **2a**. **e**, Comparison of the photo and redox properties of catalyst Δ/Λ-**Ir2** and the enolate complex **II**. Columns 2 and 3 show wavelength of maximum absorbance and emission, respectively. E^{00}, energy of the emitting excited state as calculated from the luminescence peak. Column 4 shows the one-electron redox potential of the couple oxidized sensitizer / sensitizer as determined from the peak maximum of differential pulse voltammetry. Column 5 shows the one-electron redox potential of the couple oxidized sensitizer / excited sensitizer as calculated from $E_{1/2}(PS^+/PS^*) = E_{1/2}(PS^+/PS) - E^{00}$.

e

Complex	Absorbance λ_{max}	Emission λ_{max} (E^{00})	$E_{1/2}(PS^+/PS)$	$E_{1/2}(PS^+/PS^*)$
Δ/Λ-**Ir2**	425 nm	560 nm (2.21 eV)	> +1.5 V	> –0.71 V
Enolate **II**	440 nm	550 nm (2.25 eV)	+0.51 V	–1.74 V

across half of the visible spectrum ranging from violet to green light (Fig. 4e and Supplementary Fig. 5). The visible-light absorbance of enolate complex **II** is not affected by the presence of organic bromide substrates, thus most probably ruling out the possibility that an electron donor–acceptor complex between enolate complex **II** and bromide substrate is responsible for the light absorption (Supplementary Fig. 6)[22]. It is also worth noting that an independently synthesized enolate complex **II** is catalytically competent and catalyses the photoredox reaction with an identical efficiency compared to **Ir2**, thereby supporting the notion that complex **II** has a dual function as a chiral nucleophile in the catalytic cycle and the *in situ* photosensitizer in the photoredox cycle.

Finally, two distinct variations of the outlined mechanism need to be considered (Supplementary Fig. 7). First, instead of regenerating the photooxidized sensitizer in every cycle ($PS^+ + e^- \rightarrow PS$, Fig. 3), the ketyl intermediate **III** might transfer a single electron directly to another bromide substrate, thus skipping the photoredox cycle and leading to a chain reaction. Although the direct light-dependence of the asymmetric photoactivated catalysis shown in Fig. 4c suggests that the asymmetric catalysis and photoredox cycle operate in concert at least to some extent, a contribution of the chain propagation mechanism as a function of the nature of the substrates is feasible, and might even explain the differences in photolysis times for the individual reactions[29]. The second mechanistic variation to discuss revolves around the direct reaction of the intermediate benzyl radical with the oxidized sensitizer (PS^+). However, a major contribution of this recombination process is unlikely since both reactive intermediates will not be generated in close proximity, considering that the fragmentation of the formed radical anion does not occur instantaneously. In this respect, it has been established that the life time of such radical anions significantly increases in protic solvents and with a decreasing energy of the π* orbitals[30]. This notion is supported by an experiment in which low concentrations of the radical trap TEMPO were still able to capture the intermediate benzyl radical (see Supplementary Methods), thus rendering unlikely an efficient recombination of the benzyl radical with the oxidized iridium sensitizer, and instead favouring an addition of the intermediate electron-deficient benzyl radical with the electron-rich π-bond of the iridium(III) enolate complex **II**, which is present in solution at a much higher steady state concentration.

We have reported a unique case of visible-light-induced asymmetric redox catalysis by a single, structurally simple catalyst. The two catalytic cycles are apparently connected through an intermediate iridium(III) enolate complex, formed from the initial catalyst and the 2-acyl imidazole substrate, which is not only the key nucleophilic intermediate in the asymmetric catalysis cycle but also constitutes the *in situ* generated active visible-light photosensitizer. The reaction scheme that we introduce here may serve as a blueprint for the design of other catalytic asymmetric photoredox reactions, and will most probably provide new avenues for the efficient and green synthesis of non-racemic chiral molecules.

Received 4 August; accepted 23 September 2014.

1. Walsh, P. J. & Kozlowski, M. C. *Fundamentals of Asymmetric Catalysis* (University Science Books, 2009).
2. Zeitler, K. Photoredox catalysis with visible light. *Angew. Chem. Int. Edn* **48,** 9785–9789 (2009).
3. Narayanam, J. M. R. & Stephenson, C. R. J. Visible light photoredox catalysis: applications in organic synthesis. *Chem. Soc. Rev.* **40,** 102–113 (2011).
4. Prier, C. K., Rankic, D. A. & MacMillan, D. W. C. Visible light photoredox catalysis with transition metal complexes: applications in organic synthesis. *Chem. Rev.* **113,** 5322–5363 (2013).
5. Schultz, D. M. & Yoon, T. P. Solar synthesis: prospects in visible light photocatalysis. *Science* **343,** 1239176 (2014).
6. Schmittel, M. & Burghart, A. Understanding reactivity patterns of radical cations. *Angew. Chem. Int. Edn Engl.* **36,** 2550–2589 (1997).
7. Curran, D. P., Porter, N. A. & Giese, B. *Stereochemistry of Radical Reactions: Concepts, Guidelines, and Synthetic Applications* (VCH, 1996).
8. Hopkinson, M. N., Sahoo, B., Li, J.-L. & Glorius, F. Dual catalysis sees the light: combining photoredox with organo-, acid, and transition-metal catalysis. *Chem. Eur. J.* **20,** 3874–3886 (2014).
9. Nicewicz, D. A. & MacMillan, D. W. C. Merging photoredox catalysis with organocatalysis: the direct asymmetric alkylation of aldehydes. *Science* **322,** 77–80 (2008).
10. Shih, H.-W., Vander Wal, M. N., Grange, R. L. & MacMillan, D. W. C. Enantioselective α-benzylation of aldehydes via photoredox organocatalysis. *J. Am. Chem. Soc.* **132,** 13600–13603 (2010).
11. Neumann, M., Füldner, S., König, B. & Zeitler, K. Metal-free, cooperative asymmetric organophotoredox catalysis with visible light. *Angew. Chem. Int. Edn* **50,** 951–954 (2011).
12. Cherevatskaya, M. *et al.* Visible-light-promoted stereoselective alkylation by combining heterogeneous photocatalysis with organocatalysis. *Angew. Chem. Int. Edn* **51,** 4062–4066 (2012).
13. Nagib, D. A., Scott, M. E. & MacMillan, D. W. C. Enantioselective α-trifluoromethylation of aldehydes via photoredox organocatalysis. *J. Am. Chem. Soc.* **131,** 10875–10877 (2009).
14. DiRocco, D. A. & Rovis, T. Catalytic asymmetric α-acylation of tertiary amines mediated by a dual catalysis mode: N-heterocyclic carbene and photoredox catalysis. *J. Am. Chem. Soc.* **134,** 8094–8097 (2012).
15. Tarantino, K. T., Liu, P. & Knowles, R. R. Catalytic ketyl-olefin cyclizations enabled by proton-coupled electron transfer. *J. Am. Chem. Soc.* **135,** 10022–10025 (2013).
16. Du, J., Skubi, K. L., Schultz, D. M. & Yoon, T. P. A dual-catalysis approach to enantioselective [2 + 2] photocycloadditions using visible light. *Science* **344,** 392–396 (2014).
17. Bergonzini, G., Schindler, C. S., Wallentin, C.-J., Jacobsen, E. N. & Stephenson, C. R. J. Photoredox activation and anion binding catalysis in the dual catalytic enantioselective synthesis of β-amino esters. *Chem. Sci.* **5,** 112–116 (2013).
18. Bauer, A., Westkämper, F., Grimme, S. & Bach, T. Catalytic enantioselective reactions driven by photoinduced electron transfer. *Nature* **436,** 1139–1140 (2005).
19. Müller, C., Bauer, A. & Bach, T. Light-driven enantioselective organocatalysis. *Angew. Chem. Int. Edn* **48,** 6640–6642 (2009).
20. Brimioulle, R. & Bach, T. Enantioselective Lewis acid catalysis of intramolecular enone [2+2] photocycloaddition reactions. *Science* **342,** 840–843 (2013).
21. Alonso, R. & Bach, T. A chiral thioxanthone as an organocatalyst for enantioselective [2+2] photocycloaddition reactions induced by visible light. *Angew. Chem. Int. Edn* **53,** 4368–4371 (2014).
22. Arceo, E., Jurberg, I. D., Álvarez-Fernández, A. & Melchiorre, P. Photochemical activity of a key donor–acceptor complex can drive stereoselective catalytic α-alkylation of aldehydes. *Nature Chem.* **5,** 750–756 (2013).
23. Huo, H., Fu, C., Harms, K. & Meggers, E. Asymmetric catalysis with substitutionally labile yet stereochemically stable chiral-at-metal iridium(III) complex. *J. Am. Chem. Soc.* **136,** 2990–2993 (2014).
24. Fontecave, M., Hamelin, O. & Ménage, S. Chiral-at-metal complexes as asymmetric catalysts. *Top. Organomet. Chem.* **15,** 271–288 (2005).
25. Bauer, E. B. Chiral-at-metal complexes and their catalytic applications in organic synthesis. *Chem. Soc. Rev.* **41,** 3153–3167 (2012).
26. Evans, D. A., Downey, C. W. & Hubbs, J. L. Ni(II) bis(oxazoline)-catalyzed enantioselective syn aldol reactions of *N*-propionylthiazolidinethiones in the presence of silyl triflates. *J. Am. Chem. Soc.* **125,** 8706–8707 (2003).
27. Sato, H. & Yamagishi, A. Application of the ΔΛ isomerism of octahedral metal complexes as a chiral source in photochemistry. *J. Photochem. Photobiol. C* **8,** 67–84 (2007).
28. Herrmann, A. T., Smith, L. L. & Zakarian, A. A simple method for asymmetric trifluoromethylation of *N*-acyl oxazolidinones via Ru-catalyzed radical addition to zirconium enolates. *J. Am. Chem. Soc.* **134,** 6976–6979 (2012).
29. Studer, A. & Curran, D. P. The electron is a catalyst. *Nature Chem.* **6,** 765–773 (2014).
30. Andrieux, C. P., Le Gorande, A. & Savéant, J. M. Electron transfer and bond breaking. Examples of passage from a sequential to a concerted mechanism in the electrochemical reductive cleavage of arylmethyl halides. *J. Am. Chem. Soc.* **114,** 6892–6904 (1992).

Supplementary Information is available in the online version of the paper.

Acknowledgements We acknowledge funding from the German Research Foundation (ME 1805/4-1). H.H. thanks the China Scholarship Council for a stipend.

Author Contributions E.M. conceived and coordinated the project and wrote the Letter. E.M. and H.H. designed the experiments. H.H. carried out the majority of the experiments. X.S. synthesized the new catalyst Λ-**Ir2**. C.W. contributed to the synthesis of substrates. L.Z. contributed to the synthesis and crystallization of iridium complexes. L.-A.C. provided insights into iridium enolate chemistry. P.R. performed and analysed the cyclic voltammetry under supervision of G.H. The X-ray crystallographic studies were performed by K.H. and M.M.

Author Information The X-ray crystallographic coordinates for structures of the iridium complex Λ-**Ir2**, substrate coordinated iridium complex **I** and the iridium enolate complex **II** have been deposited at the Cambridge Crystallographic Data Centre (CCDC) under deposition numbers CCDC 1014509, 1014510 and 1014876, respectively. Reprints and permissions information is available at www.nature.com/reprints. The authors declare no competing financial interests. Readers are welcome to comment on the online version of the paper. Correspondence and requests for materials should be addressed to E.M. (meggers@chemie.uni-marburg.de).